

Conductivity Equations of Protons Transporting Through 2D Crystals Obtained with the Rate Process Theory and Free Volume Concept

Tian Hao*, Yuanze Xu[‡], and Ting Hao[†]

**15905 Tanberry Dr., Chino Hills, CA 91709, USA;*

‡Xiamen University, Xicun 15-2603, Xiamen 361005, China;

†Institute of Solid State Physics, Chinese Academy of Sciences,

P. O. Box 1129, Hefei 230031, China

(Dated: April 17, 2017)

Abstract

The Eyring's rate process theory and free volume concept are employed to treat protons (or other particles) transporting through a 2D (two dimensional) crystal like graphene and hexagonal boron nitride. The protons are assumed to be activated first in order to participate conduction and the conduction rate is dependent on how much free volume available in the system. The obtained proton conductivity equations show that only the number of conduction protons, proton size and packing structure, and the energy barrier associated with 2D crystals are critical; the quantization conductance is unexpectedly predicted with a simple Arrhenius type temperature dependence. The predictions agree well with experimental observations and clear out many puzzles like much smaller energy barrier determined from experiments than from the density function calculations and isotope separation rate independent of the energy barrier of 2D crystals, etc.. Our work may deepen our understandings on how protons transport through a membrane and has direct implications on hydrogen related technology and proton involved bioprocesses.

I. INTRODUCTION

Proton transport occurs in many important natural or man-made systems like the photosynthesis in green plants, proton pumps in human body, and the production of electricity in a fuel cell. Many proton conductivity mechanisms have been proposed to explain specific rather than generic systems. Grotthuss mechanism, the proton hopping along hydrogen bonds, probably is the earliest theory proposed to explain the proton transport.¹ Structural reorganization, diffusional motions, presolvations, etc., are thought to be responsible for proton transfer, while proton tunneling is thought to be unlikely at high temperatures²⁻⁴ but was visualized in very low temperature.⁵ Single and double proton transfer is found to co-exist⁶ and protons behave very similar to electron⁷ obeying the Holstein's polaron model.

A strong interest has arisen since two dimensional atomic thick crystals like graphene and hexagonal boron nitride (hBN) were found to exhibit subatomic selectivity that can be potentially used to separate proton and its isotopes.⁸⁻¹⁰ Experimental results have shown that protons only can penetrate the monolayer of graphene and hexagonal boron nitride and unable to go through bilayer graphene, multilayer hexagonal boron nitride, and even monolayer molybdenum disulfide; With the proton was replaced with deuteron, the transportation rate is almost 10 times slower due to the large atom of deuteron.¹⁰ *Ab initio* quantum chemistry method based on density function theory has been employed to estimate the proton permeation energy barrier for understanding the proton isotope separation phenomena, predicting the separation ratio of P^+/D^+ should be about 12.⁹ Despite some degrees of success, there is a huge discrepancy between the density function predictions and the experimental results, such as the proton transport energy barrier is calculated to be 1.2 to 2.2 eV for graphene, resulting in millions of times smaller proton conductivity than experimental observations that yield 0.78 eV.⁸

For the purpose of resolving those discrepancies and explaining unexpected experimental observations, we provide a quite different theoretical framework, other than traditional density function theory, to understand the proton permeation through 2D crystals phenomena; The Eyring' rate process theory¹¹ and free volume concept¹²⁻¹⁶ are utilized to target generic proton transport systems without involving the complicated quantum mechanical calculations. Eyring's rate process theory, originated from quantum mechanics, argues that every physical or chemical phenomenon is a rate controlled process, such as chemical re-

actions, electron transfer, conductivity, viscous flows, diffusions, etc.; every process needs an activated energy to move from the initial state to the final state. Free volume theory, originated from molecular systems, is a most successful mean field theory in dealing with many-body problems. All different kinds of interactions among entities are factored into a single term, the free volume available in the systems. Since the free volume theory adequately resolves how large freedom the entities have and Eyring's rate process theory adequately describes how fast the process is, we thus integrate these two theories together to describe many seemingly unrelated systems or phenomena like glass liquids,¹⁵ colloids and polymers,¹⁷ granules,^{18,19} electrical conductivity,²⁰ and Hall Effect²¹ with great success. Proton transportation through 2D crystals should be a rate controlled process and the rate should be directly related to how much free volume available in 2D crystals.

II. THEORY

Inspired with the neutron scattering evidences for proton polaron in hydrated metal oxide proton conductors⁷ and visualization of proton tunneling at low temperatures,⁵ we further extend the idea that protons may transport very similarly to that of electrons, though proton is much heavier and larger than electron. For electron transportation, i.e., the electrical conductivity, the velocity, based on the Eyring's rate process theory, can be expressed as^{11,20}:

$$v_d = K^+ \lambda \left[\exp \frac{\alpha e \lambda E}{k_B T} - \exp \frac{-(1 - \alpha) e \lambda E}{k_B T} \right] \quad (1)$$

where v_d is the drift velocity of electrons, $K^+ = \frac{k_B T}{h} \exp(-\Delta G/RT)$, is the specific velocity rate in any direction for the undisturbed system, k_B is the Boltzmann constant, ΔG is the standard Gibbs free energy of the activation process, R is the gas constant, h is the Planck constant, λ is the distance between the initial equilibrium position to the final position, e is the charge of an electron, E is the applied electric field, T is the temperature, and α is a fraction operative directly related to the coordinate number (c_n) of an electron or molecule in the system with the relationship, $\alpha = 1/c_n$. Eq.1 is for electrons but should work for protons, too.

The parameter, λ , the distance that a proton can travel from one equilibrium position to the next, should be related to how much the free volume available for a conduction proton

in penetrating monolayer 2D crystals as illustrated in Fig. 1. Assume that the number of hexagons is N_h and the number of protons that penetrate each hexagon is N_p . Therefore, the total number of conduction protons is N_c . Apparently,

$$N_c = N_h N_p \quad (2)$$

When protons penetrate through the holes of 2D crystal, we may reasonable assume that protons may form certain packing structures. As one may know, the size of an atom is in the order of $10^{-11}m$, while that of an proton is about $10^{-15}m$, very small compared with an atom. Reasonably, an atom thick 2D crystal can still be viewed as three dimensional (3D) structure for protons. The size of the protons and how protons pack together should directly impact the free volume available for each proton, which in turn determines λ . For estimating the free volume of protons, we still utilize the method developed by Hao in dealing with the free volume of particulate systems using the inter-particle spacing (IPS) concept.²² This method has been successfully employed for estimating the free volume of particulates or electrons to derive the viscosity of colloidal suspensions, polymers, granular dry powders,^{17-19,23,24} and electron conductivity.²⁰ The IPS may be expressed as²²:

$$IPS = 2(\sqrt[3]{\phi_m/\phi} - 1)r \quad (3)$$

where r is the effective radius of an proton, ϕ_m is the maximum packing volume fraction achieved by the conduction protons, and ϕ is the volume fraction of conduction protons. Suppose that the area of the 2D crystal is A , and the thickness is t , so the volume fraction of conduction protons can be expressed:

$$\phi = \frac{\frac{4}{3}\pi r^3 N_c}{Aft} \quad (4)$$

where f is a fraction parameter between 0 and 1, thus the term Aft represents the free volume available in 2D crystal for protons to penetrate. Replacing ϕ in Eq. 3 with Eq. 4 leads to:

$$IPS = 2 \frac{(3\phi_m Aft)^{1/3} - (4\pi r^3 N_c)^{1/3}}{(4\pi N_c)^{1/3}} \quad (5)$$

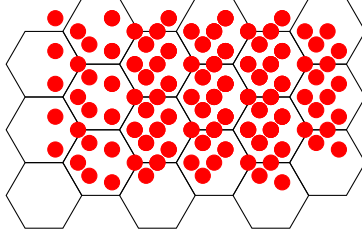


FIG. 1: Schematic illustration of protons \bullet packed in the hexagonal holes created by a 2D crystal

Adopting the similar method of treating particles or electrons in our previous publication,^{19,20,23} we still argue that a proton can move both left and right sides with the distance of IPS. Thus the equilibrium distance of a proton that can travel, λ , may be expressed as:

$$\lambda = 2IPS = 4 \frac{(3\phi_m Aft)^{1/3} - (4\pi r^3 N_c)^{1/3}}{(4\pi N_c)^{1/3}} \quad (6)$$

It is worth to mention that the volume of a proton in comparison with the available hole size per proton is critical; if the former is larger than the latter, λ will be negative and there should be no any proton transportation happening. The conductivity, σ , can be expressed as²⁵:

$$\sigma = eN_c \frac{v_d}{E} \quad (7)$$

Replacing v_d with Eq.1 leads to:

$$\sigma = \frac{eN_c K^+ \lambda}{E} \left[\exp \frac{\alpha e \lambda E}{k_B T} - \exp \frac{-(1 - \alpha) e \lambda E}{k_B T} \right] \quad (8)$$

Now, we have the free distance that a conduction electron can travel as shown in Eq.6 and need to determine the parameters N_c and K^+ . For determining N_c , one may assume that protons need to go through the Eying's activation energy barrier that is related to 2D crystal materials. Analogous to the electron conduction band theory, protons need to gain a certain energy in order to transport from the side that the protons are injected to another and participate the conduction process. The needed energy overcoming the activation barrier may be written $E_B = E_c - E_f$, where E_c is the energy of conduction band edge, and E_f is the Fermi energy of the material. As one may tell, there are a huge amount of protons in the systems with an effective concentration or activity N_{e1} initially, and only a small portion of protons is activated and penetrate through 2D crystal with the effective concentration

$N_c/(Aft)$, while the big portion of protons still remains conduction uninvolved with the effective concentration of N_{e2} . This process can be simply described as below:



Since the concentration of conduction protons should be much smaller than the initial concentration of protons, N_{e2} should be almost identical to N_{e1} . So the equilibrium constant of this process, K_c , can be written as:

$$K_c = \frac{\frac{N_c}{Aft} N_{e2}}{N_{e1}} = \frac{N_c}{Aft} \quad (9)$$

One may further assume that protons will obey the Fermi-Dirac statistics. Since the size of a proton is usually ten thousand times smaller than an atom, the proton transport through 2D crystal should be considered as 3D rather than 2D process. For a 3D conduction system, the conduction electron concentration has been theoretically obtained using Fermi-Dirac statistics^{26,27} and can be analogously applied to protons:

$$N_c/(Aft) = 2 \left(\frac{2\pi m^* k_B T}{h^2} \right)^{3/2} F_{1/2}(\epsilon) \quad (10)$$

where m^* is the effective mass of a proton, $F_{1/2}(\epsilon)$ is the Fermi-Dirac integral of order 1/2, and $\epsilon = \frac{-(E_c - E_f)}{k_B T}$. Since 2D graphene and hBN are not a good proton conductive materials and the activation energy is always needed, one may reasonable assume that E_f is well below E_c , obeying $(E_c - E_f) > 2k_B T$, the extreme non-degeneracy condition,²⁷ thus Eq.10 can be rewritten as:

$$N_c/(Aft) = 2 \left(\frac{2\pi m^* k_B T}{h^2} \right)^{3/2} \exp\left(-\frac{E_c - E_f}{k_B T}\right) \quad (11)$$

$$= 2 \left(\frac{2\pi m^* k_B T}{h^2} \right)^{3/2} \exp\left(-\frac{E_B}{k_B T}\right) \quad (12)$$

From Eq.12, one may obtain conduction proton concentration, or the parameter N_c .

Now we have to determine the parameter K^+ , the specific velocity rate in any direction for the undisturbed system, which can be expressed below^{11,21}:

$$K^+ = K_c \frac{1}{\delta} \left(\frac{k_B T}{2\pi m^*} \right)^{1/2} \quad (13)$$

where δ is the length of top activation barrier. Replacing K_c in Eq. 13 with Eq. 9 and $2\pi m^*$ with Eq. 12 leads to:

$$K^+ = \frac{N_c}{Aft} \frac{1}{\delta} \left(\frac{k_B T}{2\pi m^*} \right)^{1/2} = \frac{\sqrt[3]{2} k_B T}{\delta h} \left(\frac{N_c}{Aft} \right)^{2/3} \exp\left(-\frac{E_B}{3k_B T}\right) \quad (14)$$

Now we have everything and the proton conductivity Eq. 8 can be rewritten as:

$$\sigma = \frac{2^{5/3} e N_c^{4/3} k_B T [(3\phi_m)^{1/3} - (\frac{4\pi r^3 N_c}{Aft})^{1/3}]}{\delta h E (\pi Aft)^{1/3}} \exp\left(-\frac{E_B}{3k_B T}\right) \left[\exp\frac{\alpha e \lambda E}{k_B T} - \exp\frac{-(1-\alpha)e \lambda E}{k_B T} \right] \quad (15)$$

Eq. 15 gives a complicated relationship but can be simplified further, as proton conduction experiments are typically performed at higher temperatures and may meet the condition $\alpha e \lambda E < k_B T$. Using the approximation $e^x \approx 1 + x$ when $x < 1$, one may obtain:

$$\begin{aligned} \sigma &= \frac{e^2}{h} \frac{8N_c}{\delta} \left(\frac{3}{\pi}\right)^{2/3} \left[(\phi_m)^{1/3} - \left(\frac{4\pi r^3 N_c}{3Aft}\right)^{1/3} \right]^2 \exp\left(-\frac{E_B}{3k_B T}\right) \\ &= \nu \frac{e^2}{h} \end{aligned} \quad (16)$$

where $\nu = \frac{8N_c}{\delta} \left(\frac{3}{\pi}\right)^{2/3} \left[(\phi_m)^{1/3} - \left(\frac{4\pi r^3 N_c}{3Aft}\right)^{1/3} \right]^2 \exp\left(-\frac{E_B}{3k_B T}\right)$, a parameter only related to the material properties of 2D crystals.

III. RESULTS

As one may already notice, the amazing feature of Eq. 16 is that the proton conductivity is predicted to show conductance quantization typically dubbed the Hall effect for electron conductivity. The highly reproducible experimental data for different samples even with different proton injection materials but same 2D crystals⁸ may support that Eq. 16 is indeed valid. In addition, the "proton Hall effect" has been experimentally observed in ice²⁸ and hydrogen in Palladium,²⁹ further validating the predictions of Eq. 16.

Clearly, the proton conductivity has Arrhenius type relationship with temperature, which is consistent with the experimental observations.⁸ The energy barrier for proton conduction is predicted to be one third of the energy needed for activating protons from the ground state to conduction state. This interesting prediction may provide some clues on the puzzles why the calculated energy barrier is much larger than the experimental derived values, 1.2 ~ 2.2 and 0.7 or 0.9 eV calculated from *ab initio* molecular dynamics simulations^{8,30-33} vs. 0.78 and 0.3 eV determined from experimental results for graphene and hBN, respectively.⁸

Fig.2 shows the experimental data points taken from the literature⁸ and regressed very well with Eq. 16. The obtained energy barriers based the experimental data and Eq. 16 are $E_B = 2.49 \pm 0.040eV$ for monolayer graphene and $E_B = 1.17 \pm 0.016eV$ for monolayer hBN, which are more reasonably close to the theoretical calculated values, especially when all factors like the structural optimization, the role of the solvent, surface curvature, and proton transport through hydrogenated samples are taken into considerations.³³ Again, the discrepancy between the theoretical calculations and experimental values are mainly caused by the fact that the former should be 3 times higher than the latter, as indicated by Eq. 16; all corrections made for lowering energy barrier to be consistent with experimental data actually go to the opposite direction and push the calculated values even higher.³³

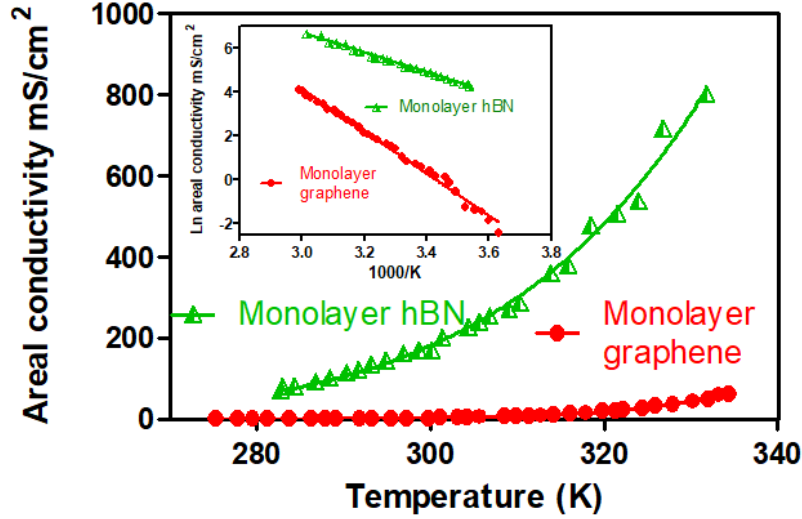


FIG. 2: The areal conductivity of proton transport through monolayer graphene is plotted against the temperature. The data points are taken from Figure 2 of the reference⁸ and the curved lines are regressed with Eq.16 of the goodness $R^2 = 0.9968$ for monolayer graphene and 0.9915 for monolayer hBN. The inset is the natural logarithm of areal conductivity vs. T^{-1} with a linear fit of the goodness $R^2 = 0.9920$ for monolayer graphene and 0.9957 for monolayer hBN, which yields the conductivity energy barrier $E_B = 2.49 \pm 0.040eV$ for monolayer graphene and $E_B = 1.17 \pm 0.016eV$ for monolayer hBN, in line with theoretical calculations.

Eq. 16 tells that the conductivity is dependent on the size of the particles penetrating 2D

crystals. For a same 2D crystal, taking proton and deuteron as an example, the conductivity difference between proton and deuteron will be resulted from the radius and the number of conduction particles. The data from NIST indicate that the radius of proton and deuteron is 0.8751 and 2.1413 fm ,³⁴ respectively, though the latest measurement gives 0.8356 and 2.1277 fm .³⁵ Assume that both of protons and deuterons may take random close packing structure when penetrating 2D crystals. Many articles have proved, both experimentally and theoretically, the maximum packing fraction of random close packing is about 0.63, most times independent of particle sizes when particle interactions are negligible; However, particle size impact cannot be ignored if particle surface area or surface energy is large and the container sizes are comparable with the particle sizes.³⁷⁻⁴¹ The lattice constants of both graphene and hBN are about 0.25 nm , very larger in comparison with the sizes of protons and deuterons.⁴² Therefore the surface area or energy impact cannot be neglected. An equation correlated the packing fraction, ϕ , with the particle size of monospheres has been developed⁴³:

$$\phi = \phi_{tm} \left(\frac{1}{1 + 3k/r} \right) \quad (17)$$

where r is the radius of particles, and ϕ_{tm} is the true maximum packing fraction when particle surface impact is considered, and k is a constant scaling the ratio of volume to surface area of particles and independent of particle sizes. Assume both protons and deuterons are perfect spheres and use the radius ratio of deuteron to proton about 2.5, an average value from NIST and the literature,³⁵ one may easily find that the packing fraction of deuterons, ϕ_D , and that of protons, ϕ_P , based on Eq. 17, have a relationship:

$$\phi_D = 1.429\phi_P \quad (18)$$

calculated when protons are used as a reference and $k = \frac{\frac{4}{3}\pi r_P^3}{4\pi r_P^2} = \frac{r_P}{3}$, the ratio of proton volume to surface area. When particle sizes increase from protons to deuterons, the extra packing volume created by deuterons is analogously considered to be a thick layer attached on proton particle surfaces but remain a same k , very similar to the cell model employed for calculating the IPS.²² Eq. 18 therefore can be re-written as in term of particle volumes:

$$\frac{4}{3}\pi r_D^3 N_{cD} = 1.429 \times \frac{4}{3}\pi r_P^3 N_{cP} \quad (19)$$

$$\frac{N_{cP}}{N_{cD}} = 0.67 \left(\frac{r_D}{r_P} \right)^3 \quad (20)$$

where r_P and r_D , N_{cP} and N_{cD} are the radius and the number of conduction proton and deuteron, respectively. According to Eq. 16, the conductivity ratio of proton to deuteron is:

$$\frac{\sigma_P}{\sigma_D} \approx \frac{N_{cP}}{N_{cD}} = 10.93 \quad (21)$$

Clearly, Eq. 21 shows that the conductivity ratio of proton to deuteron is independent of many seemingly important factors like 2D crystals, the energy barriers, the sample sizes, experimental setups, etc., which are in great consistency with experimental observations.¹⁰ Amazingly, the predicted conductivity ratio of proton to deuteron is about 10.93, in a very good agreement with ~ 10 obtained experimentally.¹⁰ Of course, our prediction is greatly dependent on the precision of radius data that need further refinements,³⁵ however, it will not change too much.

IV. DISCUSSION

Two important assumptions are employed in deriving proton conduction equations in this article. They are extreme non-degeneracy condition that an energy needed to activate protons for participating conduction process meets $(E_c - E_f) > 2k_B T$, and the relatively high temperature condition that $\alpha e \lambda E < k_B T$. They are very reasonable assumptions in term of how typical proton transport experiments are performed. Both Eq. 15 and 16 are pretty general and can be applied to many systems. When temperature is low enough that $\alpha e \lambda E > k_B T$, Eq. 15 should be used. Similar to electron pairing at low temperatures, if protons are pairing where $\alpha = 1$, thus Eq. 15 will be rewritten as:

$$\sigma = \frac{2^{5/3} e N_c^{4/3} k_B T [(3\phi_m)^{1/3} - (\frac{4\pi r^3 N_c}{Aft})^{1/3}]}{\delta h E (\pi Aft)^{1/3}} \exp(-\frac{E_B - 3e\lambda E}{3k_B T}) \quad (22)$$

under the condition that $\exp(\frac{e\lambda E}{k_B T}) \gg 1$. The energy barrier value determined experimentally should be much lower than the calculated energy barrier, E_B .

Note that conductivity equations derived in this article are not specifically limited to protons and should be applicable to any other charge carriers. the sign of elementary charge e should be changed accordingly, for example, changed to positive for protons in all related equations.

V. CONCLUSION

In summary, the Eyring's rate process theory and free volume concept are successfully employed to treat the proton transport through 2D crystals. The obtained conductivity equations show the conductance quantization similar to the Hall effect associated with electrons; The conductivity is only related to the number and size of conduction protons, packing structures of protons, and the energy barrier from 2D crystals; It is independent of proton injecting materials and sample sizes. Our equations resolve several puzzles, like why the energy barrier obtained experimentally is much smaller than theoretical values calculated with density function theory, why deuterons transport about 10 times slower than protons, and why the isotope effect is independent of 2D crystal membranes or the energy barrier, etc.. Our theory presents an excellent agreement with the experimental observations, deepening our understandings on proton transport through 2D crystals and shedding light on how to optimize proton transport systems.

The theoretical framework utilized in this article is same as the ones employed to treat colloidal suspensions,²⁴ polymers,^{15,24} granular powders,^{18,19} electrical conductivity,²⁰ Hall effect,²¹ and even our universe.³⁶ The success of current work extends our previous idea that the multi-scale systems spanning from the microscopic to the macroscopic worlds could be treated with a single theoretical formulation, the combination of the Eyring rate process and free volume theories.

Acknowledgments

The author sincerely appreciate many colleagues' and reviewers' feedback and comments for substantially improving the readability and rationality of this article.

¹ S. Cukierman, Et tu Grotthuss! and other unfinished stories, *Biochimica et Biophysica Acta*, 2006, **1757** (8), 876-885

² K. Kreue, Proton Conductivity: Materials and Applications, *Chem. Mat.*, 1996, **8**, 610-641

³ L. Vilčiauskas, M. E. Tuckerman, G. Bester, S. J. Paddison, and K. Kreuer, The mechanism of proton conduction in phosphoric acid, *Nature Chem.*, 2012, **4**, 461-466

- ⁴ V. Quaranta, M. Hellström, J. Behler, Proton-Transfer Mechanisms at the Water-ZnO Interface: The Role of Presolvation, *J. Phys. Chem. Lett.*, 2017, **8**(7), 1476-1483
- ⁵ X. Meng, J. Guo, J. Peng, J. Chen, Z. Wang, J. Shi, X. Li, E. Wang, Y. Jiang, Direct visualization of concerted proton tunnelling in a water nanocluster, *Nature Phys.*, 2015, **11**, 235–239
- ⁶ B. Xiao, J. Cheng, and X. Yu, Double-proton transfer mechanism in 1,8-dihydroxydibenzo[a,c]phenazine: a TDDFT and ab initio study, *Theor. Chem. Acc.*, 2015, **134**, 111
- ⁷ A. Braun and Q. Chen, Experimental neutron scattering evidence for proton polaron in hydrated metal oxide proton conductors, *Nature Comm.*, 2017, **8**, 15830
- ⁸ S. Hu, M. Lozada-Hidalgo, F. C. Wang, A. Mishchenko, F. Schedin, R. R. Nair, E. W. Hill, D. W. Boukhvalov, M. I. Katsnelson, R. A. W. Dryfe, I. V. Grigorieva, H. A. Wu, and A. K. Geim, Proton transport through one-atom-thick crystals, *Nature*, 2017, **516**, 227-230.
- ⁹ Q. Zhang, M. Ju, L. Chen, and X. Zen, Differential Permeability of Proton Isotopes Through Graphene and Graphene Analogue Monolayer, *J. Phys. Chem. Lett.*, 2016, **7**(17), 3395–3400.
- ¹⁰ M. Lozada-Hidalgo, S. Hu, O. Marshall, A. Mishchenko, A. N. Grigorenko, R. A. W. Dryfe, B. Radha, I. V. Grigorieva, and A. K. Geim, Sieving Hydrogen Isotopes through Two-dimensional Crystals, *Science*, 2016, **351**, 68-70.
- ¹¹ S. Glasstone, K. Laidler, and H. Eyring, *The Theory of Rate Process*, McGraw-Hill, 1941
- ¹² M. H. Cohen and D. Turnbull, Molecular transport in liquids and glasses, *J. Chem. Phys.*, 1959, **31**, 1164–1169
- ¹³ D. Turnbull and M. H. Cohen, Free-Volume Model of the Amorphous Phase: Glass Transition, *J. Chem. Phys.*, 1961, **34**, 120–124
- ¹⁴ J. C. Dyre, Source of non-Arrhenius Average Relaxation Time in Glass-forming Liquids, *J. Non-Crystalline Solids*, 1998, **235-237**, 142-149
- ¹⁵ T. Hao, Unveiling the Relationships among the Viscosity Equations of Glass Liquids and Colloidal Suspensions for Obtaining Universal Equations with the Generic Free Volume Concept, *Phys. Chem. Chem. Phys.*, 2015, **17**, 21885-21893
- ¹⁶ H. Fujita, Notes on Free Volume Theories, *Polymer J.*, 1991, **23**, 1499-1506
- ¹⁷ T. Hao, Viscosities of liquids, colloidal suspensions, and polymeric systems under zero or non-zero electric field, *Adv. Coll. Interf. Sci.*, 2008, **142**, 1-19
- ¹⁸ T. Hao, Derivation of stretched exponential tap density equations of granular powders, *Soft*

- Matter*, 2015, **15**, 3056-3061
- ¹⁹ T. Hao, Tap density equations of granular powders based on the rate process theory and the free volume concept, *Soft Matter*, 2015, **11**, 1554-1561
- ²⁰ T. Hao, Electrical Conductivity Equations Derived with the Rate Process Theory and Free Volume Concept, *RSC Adv.*, 2015, **5**, 48133-48146
- ²¹ T. Hao, Integer, Fractional, and Anomalous Quantum Hall Effect Explained with Eyring's Rate Process Theory and Free Volume Concept, *Phys. Chem. Chem. Phys.*, 2017, **19**, 6042-6050
- ²² T. Hao, and R. E. Riman, Calculation of Interparticle Spacing in Colloidal Systems, *J. Coll. Interf. Sci.* , 2006, **297**, 374-377
- ²³ T. Hao, Analogous Viscosity Equations of Granular Powders Based on Eyring's Rate Process Theory and Free Volume Concept, *RSC Adv.*, 2015, **5**, 95318-95333
- ²⁴ T. Hao, *Electrorheological Fluids: The Non-aqueous Suspensions*, Elsevier, December 19, 2005
- ²⁵ C. Kittel, *Introduction to Solid State Physics*, Wiley, November 11, 2004
- ²⁶ R. Kim and M. Lundstrom, Notes on Fermi-Dirac Integrals, arXiv:0811.0116, 2008
- ²⁷ E. Fred Schubert, *Physical Foundations of Solid-State Devices*, 2015.
- ²⁸ B. Bullemer and N. Riehl, Hall effect on protons in ice, *Phys. Lett.* , 1966, **22**, 411-412
- ²⁹ A. H. Verbruggen, R. Griessen, and J. H. Rector, Hall Voltage Induced by Hydrogen Diffusion in Palladium, *Phys. Rev. Lett.* , 1984, **52**, 1625-1628
- ³⁰ W. L. Wang and E. Kaxiras, Graphene hydrate: theoretical prediction of a new insulating form of graphene, *New J. Phys.* , 2010, **12**, 125012
- ³¹ M. Miao, M. B. Nardelli, and Y. Liu, First principles study of the permeability of graphene to hydrogen atoms, *Phys. Chem. Chem. Phys.*, 2013, **15**, 16132-16137
- ³² L. Tsetseris and S. T. Pantelides, Graphene: an impermeable or selectively permeable membrane for atomic species? *Carbon*, 2014, **67**, 58-63
- ³³ J. M. H. Kroes, A. Fasolino, and M. I. Katsnelson, Density functional based simulations of proton permeation of graphene and hexagonal boron nitride, *Phys. Chem. Chem. Phys.* , 2017, **19**, 5813-5817
- ³⁴ The 2014 CODATA Recommended Values of the Fundamental Physical Constants, <http://physics.nist.gov/cuu/Constants/index.html>, National Institute of Standards and Technology, Gaithersburg, MD, US
- ³⁵ R. Pohl, F. Nez, L. M. P. Fernandes, et.al, Laser spectroscopy of muonic deuterium, *Science*,

2016, **353**, 669-673

- ³⁶ T. Hao, Y. Xu, and Ting Hao, Exploring the Inflation and Gravity of the Universe with Eyring's Rate Process Theory and Free Volume Concept, *virra: 1701.0003*, 2017
- ³⁷ L. Burtseva, B. V. Salas, F. Werner, V. Petranovskii, Packing of monosized spheres in a cylindrical container: Models and approaches, *Rev. Mex. Fis.* , 2015, **61**, 20–27
- ³⁸ W. Zhang, K. E. Thompson, A. H. Reed, and L. Beenken, Relationship between packing structure and porosity in fixed beds of equilateral cylindrical particles, *Chem. Eng. Sci.*, 2006, **61**, 8060-8074
- ³⁹ C. D. Zangmeister, J. G. Radney, L. T. Dockery, J. T. Young, X. Ma, R. You, and M. R. Zachariah, Packing density of rigid aggregates is independent of scale, *PANS*, 2014, **111**, 9037–9041
- ⁴⁰ R. P. Zou and A. B. Yu, The packing of spheres in a cylindrical container: the thickness effect, *Chem. Eng. Sci.* , 1995, **50**, 1504-1507
- ⁴¹ A. M. Ribeiro, P. Neto, and C. Pinho, Mean Porosity and Pressure Drop Measurements in Packed Beds of Monosized Spheres: Side Wall Effects, *Int. Rev. Chem. Eng.*, 2010, **2**, 40-46
- ⁴² J. Wang, F. Ma, and M. Sun, Graphene, hexagonal boron nitride, and their heterostructures: properties and applications, *RSC Adv.* , 2017, **7**, 16801-16822
- ⁴³ R. F. Fedors, A Relationship between Maximum Packing of Particles and Particle Size, *Powder Tech.* , 1979, **22**, 71-76